Active Flow Control Over a Wing Model Using Synthetic-Jet-Actuator Arrays

Hui Tang, Pramod Salunkhe, Jiaxing Du and Yanhua Wu

Abstract In this study, synthetic-jet-actuator (SJA) arrays were designed, implemented, and tested on a straight-wing model for flow separation control. First, the characteristics of a single SJA were determined. The jet velocity appears a peak between 400 and 500 Hz, which corresponds to the SJA's Helmholtz resonance frequency. Second, two arrays of such SJAs were implemented at different chordwise locations on a straight-wing model. Force balance measurements and power spectrum analysis showed that both SJA arrays are able to effectively delay flow separation, with the front SJA array more effective than the rear one. For the front array, the improvement in C_L and C_D was 27.4 % and 19.6 %, respectively.

Keywords Synthetic jet · Synthetic-jet-actuator array · Active flow control · UAV

1 Introduction

Synthetic jet (SJ) technology has been proved to be a promising active flow control means in aeronautical applications, including flow separation control (Amitay and Glezer 2002; Zhong et al. 2007), mixing control (Pavlova et al. 2008), and turbulence control (Rathnasingham and Breuer 2003). As shown in Fig. 1, a typical synthetic jet actuator (SJA) consists of a cavity with an oscillatory diaphragm on one side and an orifice on another side. The oscillation of the diaphragm generates a succession of vortex structures that propagate away from the orifice, forming a so-called synthetic jet. Due to its well-known zero-net-mass-flux and compact

H. Tang (✉) · P. Salunkhe · J. Du · Y. Wu
School of Mechanical and Aerospace Engineering, Nanyang Technological University, Singapore, Singapore
e-mail: htang@ntu.edu.sg

Y. Zhou et al. (eds.), *Fluid-Structure-Sound Interactions and Control*,
Lecture Notes in Mechanical Engineering, DOI: 10.1007/978-3-642-40371-2_16,

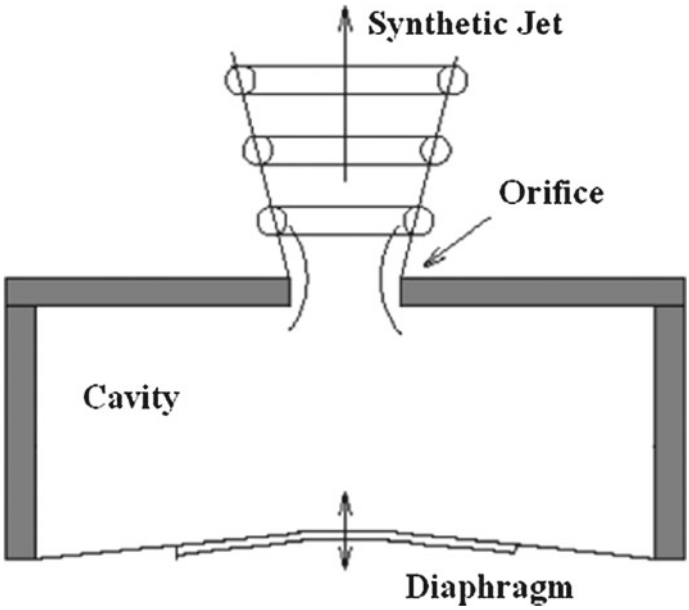

Fig. 1 Schematic of a SJA

features, SJA can be easily implemented in arrays to achieve better flow control effects. As a study toward realizing active flow control for unmanned aerial vehicles (UAVs) by applying the SJ technology, the current investigation aims to design and deploy suitable SJA arrays to control the possible flow separation over a straight-wing model and hence enhance its aerodynamic performance. In addition, an experimental framework will be established for the investigation of the active flow control effectiveness and efficiency of SJA arrays on UAV wings.

2 Test Rig Setup and Instrumentation

Experiments were carried out in a subsonic closed-loop wind tunnel at a speed of 10 m/s. The test section size of the wind tunnel is 0.8 m (W) × 0.8 m (H) × 2 m (L). The wing model used in this study is based on the low-speed LS(1)-0421MOD airfoil, with chord length $c = 180$ mm and span $b = 255$ mm. In the present study, a new design of piezoelectric-driven SJA is proposed as shown in Fig. 2. It consists of four 20-mm-diameter piezoelectric ceramic disks attached to its four sidewalls. An O-ring is placed right above the opening on its top for a leak-proof fit. Multiple such SJAs can be arrayed and incorporated inside the cavity that is formed within the wing model. The orifice of the SJA consists of five 1-mm-diameter holes in a row on the wing model, with a distance of 1 mm

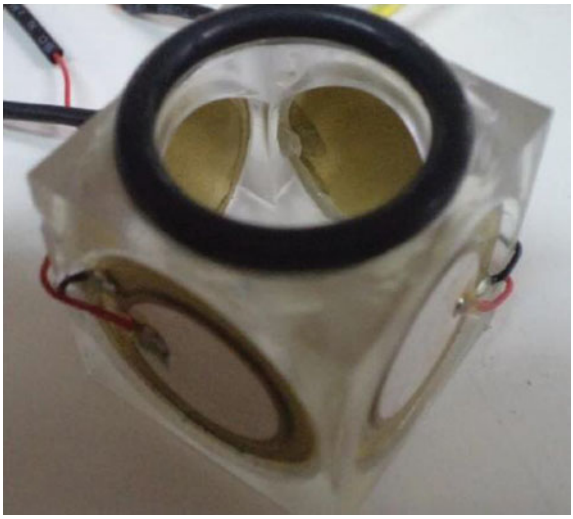

Fig. 2 Current SJA design

between the successive holes. Ten such orifices were then arranged by keeping a 25-mm distance between each orifice. The array of SJAs was placed inside the cavity in such a way that each orifice is open to its respective SJA cavity.

In the present studies, two arrays of SJAs were incorporated in the wing model as shown in Fig. 3, each consisting of ten SJAs aligned in the spanwise direction. These two arrays are located at 23 % of the chord (denoted as front array) and 43 % of the chord (denoted as rear array) from the leading edge. A six-component force balance was used for the lift and drag measurement.

The SJAs were driven using a power amplifier (EPA-104 from Piezo Systems Inc.). The maximum output voltage is ±200 Vp, and the maximum output power is 40 Wp. Due to the limited power capacity of the amplifier and the large number of

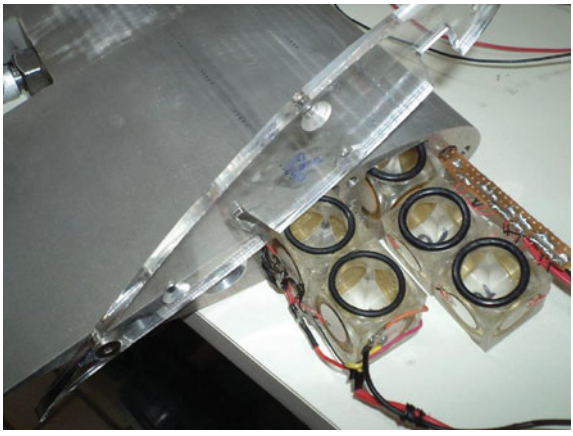

Fig. 3 Two SJA arrays to be installed

the piezoelectric diaphragms (40 in total for one array), only one SJA array was driven at a time with a maximum frequency of 600 Hz. A function generator was used to generate the sinusoidal waveform and output voltages at various frequencies. The velocity measurement at various chordwise locations was carried out using a hot-wire anemometer (CTA 54T30 from Dantec Dynamics). A one-dimensional probe, 55P16, was used for this purpose. For spectral measurements, the hot-wire probe was placed 8 mm above the suction surface of the wing and traversed at three different locations, viz. 33 %, 50 %, and 67 % of the chord.

The present study aims to investigate the effect of the proposed SJA arrays on the flow separation control effectiveness on the wing model. Various measurement techniques were employed, including velocity measurements using a hot-wire anemometer and lift and drag measurements using a force balance.

3 Results and Discussions

The SJ velocity as generated by a single SJA was measured in quiescent conditions using a hot-wire anemometer. The hot-wire probe was placed 1 mm directly above one of the SJA's five holes. In this test, the four diaphragms were operated in phase at different voltages, namely, 100, 150, and 200 Vp. Figure 4 shows the variation of SJ velocity with frequency at various voltages. As expected, the jet peak velocity increases as the driving voltage increases, with the maximum velocity reaching about 7 m/s. All three curves demonstrate a velocity peak between 400 and 500 Hz. Since this frequency range is far below the diaphragm's natural frequency (1,500 Hz), it is believed that this peak corresponds to the SJA's Helmholtz resonance frequency. The test results indicate that the current SJA needs to be operated around its Helmholtz resonance frequency for higher jet velocities and hence better control effects if applied on the wing model.

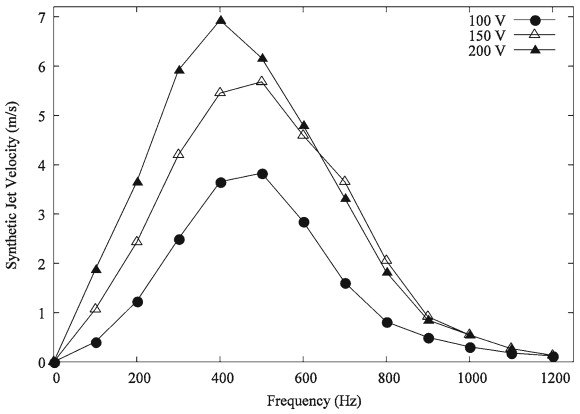

Fig. 4 SJ velocity against frequency

The wing model with the two SJA arrays embedded was tested in the wind tunnel at a constant wind speed 10 m/s, the typical flight speed of small UAVs. The aerodynamic forces exerted on the wing model with and without the actuation of the SJA arrays at different angles of attack (AOAs) were measured using a six-component force balance. The SJA arrays were driven with the voltage of 200 Vp at three different frequencies, i.e., 200, 400, and 600 Hz.

Figure 5 shows the variation of lift coefficient (C_L) and drag coefficient (C_D) against AOAs, with and without SJA actuation. It was observed that after switching on the SJA arrays, C_L increased substantially at higher AOAs, whereas C_D decreased throughout the entire AOA range. The change in C_L is believed to be associated with the delay of the flow separation on the suction surface of the wing model, indicating the SJA arrays are able to effectively delay the flow separation. It was also observed that the improvement in C_L and C_D was significant for actuation at 400 and 600 Hz compared to at 200 Hz over the without actuation case. The small improvement at 200 Hz may be attributed to the relatively low jet

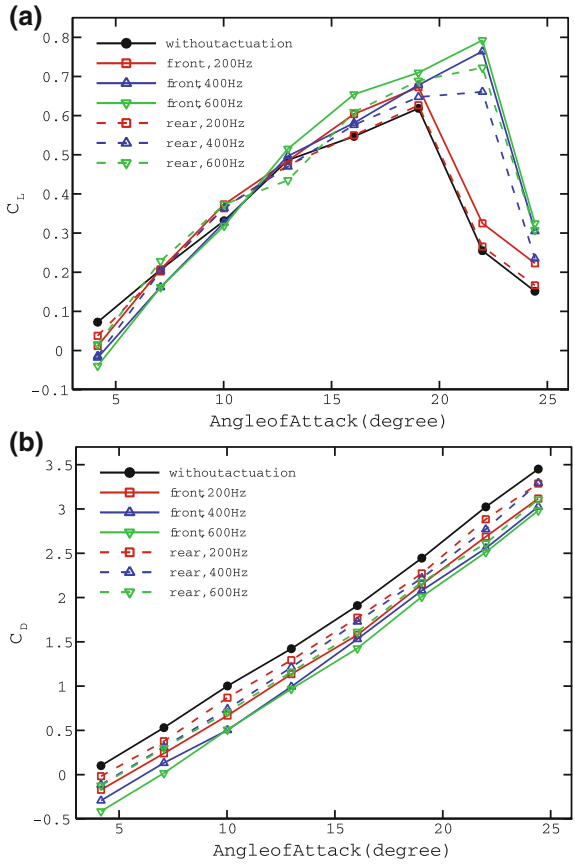

Fig. 5 Variation of **a** C_L and **b** C_D against AOA, with and without the actuation of SJA arrays

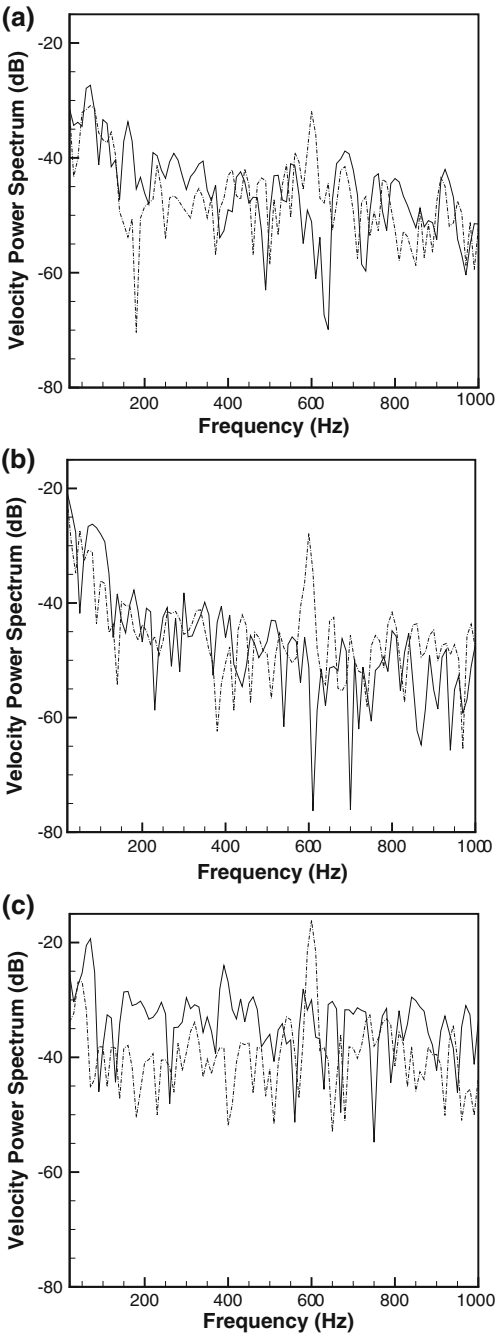

Fig. 6 Power spectra of the velocity magnitude with and without the actuation of the front SJA array at **a** 0.33*c*, **b** 0.5*c*, and **c** 0.67*c*. The AOA of the wing model is 18°. *Solid line* spectra without actuation; *Dotted lines* spectra with SJA actuation at 600 Hz

velocity produced by the SJA arrays. From the hot-wire measurements shown in Fig. 4, the maximum SJ velocity at 200 Hz is only about 3.7 m/s, whereas it is 6.9 m/s at 400 Hz and 4.8 m/s at 600 Hz.

The flow separation control effectiveness of the two SJA arrays was also compared. At 600 Hz, for example, when the front array was in operation, the maximum C_L increased from 0.62 to 0.79 resulting in a 27.4 % improvement over the without actuation case, and the average C_D reduction was found to be 0.48, a 19.6 % improvement if normalized by the C_D value at the stall AOA. For the rear SJA array, the improvement in the maximum C_L and C_D was found to be 16.1 % and 11.9 %, respectively. These numbers indicate that the front SJA array performs better than the rear SJA array.

Power spectra of the velocity magnitude fluctuations were measured with and without the actuation of the front SJA array at three chordwise stations ($0.33c$, $0.5c$, and $0.67c$) using a hot-wire anemometer. Figure 6 shows the spectra below 1 kHz, which represent large-scale motions associated with the flow separation. When the SJA array was not in operation, the mean power spectra at $0.33c$ and $0.5c$ were in the similar range between −55 dB and −45 dB, whereas they were significantly higher at $0.67c$ between −30 dB and −40 dB. This reveals that flow separation at the current AOA of 18° initiates after the second station 0.5 c, and the large-scale flow structures associating with flow separation dominate the rear portion of the suction surface. When the SJA array was actuated, a moderate improvement in flow separation control in terms of damping out of disturbances was observed at first two stations. For the third station $0.67c$, however, pronounced reduction in the power spectra was observed, indicating the previous large-scale flow structures were destroyed and the flow separation was successfully damped.

The flow separation delay indicated by the force measurements and power spectrum analysis may be attributed to two mechanisms: (1) the complex vortex structures produced by the interaction between the SJs and the cross flow bring the outer high-momentum flow into the wing-surface boundary layer; and (2) the oscillation of SJs triggers the instability of the separated-flow shear layer, breaking down large flow structures into small ones in the separated region. Both mechanisms are able to increase the momentum of the boundary layer and hence delay the flow separation. To determine which one is the dominant mechanism, however, further investigations are needed.

4 Conclusions

The present study proposed a new design of SJA arrays for the flow separation control over a straight-wing model. First, a single SJA was investigated to determine its characteristics. The jet velocity appears a peak between 400 and 500 Hz, which corresponds to the SJA's Helmholtz resonance frequency, and gives the preferred operational frequency range. Second, two arrays of such SJAs were implemented at different chordwise locations on a straight-wing model.

Force balance measurement results show that the SJA arrays can effectively increase the stall angle and maximum lift and reduce the drag at 400 and 600 Hz, whereas they marginally improve the aerodynamic performance of the wing model at 200 Hz due to the relatively low jet velocity. The power spectrum analysis confirmed these findings. It was also found that the front SJA array (at 0.23c from the leading edge) is more effective than the rear SJA array (at 0.43c).

References

Amitay M, Glezer A (2002) Role of actuation frequency in controlled flow reattachment over a stalled airfoil. AIAA J 40:209–216

Zhong S, Jabbal M, Tang H et al (2007) Toward the design of synthetic-jet actuators for full-scale flight conditions. Flow, Turbul Combust 78:283–307. doi:10.1007/s10494-006-9064-0

Pavlova AA, Otani K, Amitay M (2008) Active control of sprays using a single synthetic jet actuator. Int J Heat Fluid Fl 29:131–148. doi:10.1016/j.ijheatfluidflow.2007.06.004

Rathnasingham R, Breuer KS (2003) Active control of turbulent boundary layers. J Fluid Mech 495:209–233. doi:10.1017/S0022112003006177